Check for updates

European Journal of Organic Chemistry

EurJOC
European Journal of Organic Chemistry

Chemistry Europe
European Chemical Societies Publishing

RESEARCH ARTICLE OPEN ACCESS

Electrochemical Dehydration of Carboxamides to Their Nitriles

Enrico Lunghi[1] | Annemijn M. van Koten[1] | Siegfried R. Waldvogel[1,2]

[1]Department of Electrosynthesis, Max-Planck-Institute for Chemical Energy Conversion, Mülheim an der Ruhr, Germany | [2]Karlsruhe Institute of Technology, Institute of Biological and Chemical Systems – Functional Molecular Systems (IBCS–FMS), Karlsruhe, Germany

Correspondence: Siegfried R. Waldvogel (siegfried.waldvogel@cec.mpg.de)

Received: 30 November 2025 | **Revised:** 18 December 2025 | **Accepted:** 9 January 2026

Keywords: dehydration | electrocatalysis | electrochemistry | nitriles | sustainable chemistry

ABSTRACT

An efficient electrochemical strategy for the dehydration of carboxamides to their corresponding nitriles is reported. This method replaces conventional dehydrating reagents with a thiocyanate-mediated electrochemical activation, providing a safer, milder, and more sustainable alternative. Under optimized conditions in an undivided cell, 18 examples of aromatic and aliphatic carboxamides were smoothly converted to the corresponding nitriles at ambient temperature in good-to-excellent yields (up to 84%). Hexafluoroisopropanol proved to be essential for reaction efficiency, while tetrabutylammonium thiocyanate acted as a redox mediator, as confirmed by cyclic voltammetry studies, which revealed an EC-type-mediated oxidation process. The method demonstrates broad functional-group tolerance, including halogenated, methoxylated, and sterically hindered substrates, as well as complex molecules derived from pharmaceuticals and natural products. Importantly, the protocol was successfully scaled up eightfold with minimal loss in yield, illustrating its robustness and practical applicability. Mechanistically, anodic oxidation of thiocyanate generates highly reactive species that activate the amide functionality, leading to nitrile formation via an oxidative dehydration pathway, while hydrogen evolution occurs at the cathode. This work expands the synthetic utility of electrochemical dehydration reactions and offers a valuable, environmentally responsible route to nitrile-containing compounds of broad relevance for pharmaceuticals, agrochemicals, and materials science.

1 | Introduction

The nitrile functionality represents a highly valuable structural motif in organic synthesis, as it constitutes a key intermediate and entity in countless bioactive molecules and advanced materials [1]. Nitriles are ubiquitous in pharmaceuticals, agrochemicals, and natural products [2], and serve as versatile precursors to carboxylic acids, heterocycles, and as unique substrates for electrochemical reduction to primary amines (Scheme 1) [3, 4]. Traditionally, access to nitriles has relied on dehydrative protocols utilizing harsh reagents such as phosphorus oxychloride, thionyl chloride, or strong carbodiimides [5], conditions that often generate toxic waste [6], pose operational hazards, and offer limited functional-group tolerance [7]. Alternative approaches, including transition-metal-catalyzed cyanation [8] and oxidative ammoxidation [9], typically require prefunctionalized substrates, costly catalysts, or hazardous cyanide sources [10]. A mild way of dehydration of oximes can be conducted either by electrochemical [11, 12] or enzymatic methods [13–15]. Although these methods are cyanide free, they rely on the corresponding aldehydes and hydroxylamine as energetic compound. By contrast, carboxamides are readily accessible, bench-stable, and environmentally benign precursors for several chemical transformations, including the electrochemical Hoffman rearrangement [16, 17], rendering their direct dehydration to nitriles an attractive strategy within sustainable synthesis [6]. Electrochemical dehydration of carboxamides therefore represents a promising and underdeveloped approach

Enrico Lunghi and Annemijn M. van Koten contributed equally to this work.

This is an open access article under the terms of the Creative Commons Attribution License, which permits use, distribution and reproduction in any medium, provided the original work is properly cited.

© 2026 The Author(s). *European Journal of Organic Chemistry* published by Wiley-VCH GmbH.

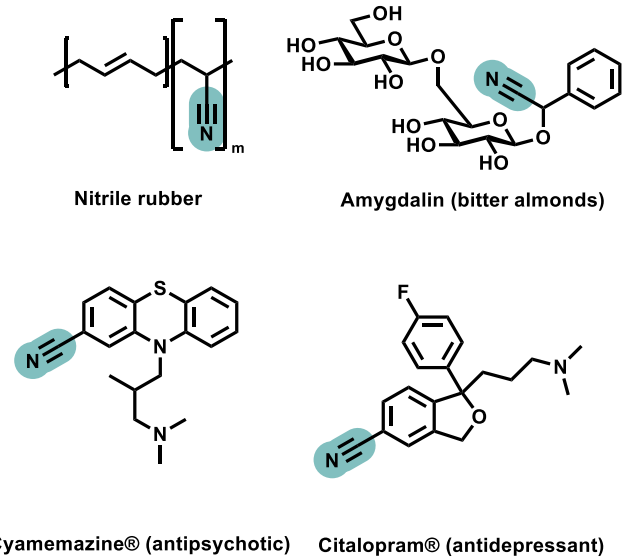

SCHEME 1 | Representative examples of nitrile-containing compounds, highlighting the prevalence of the nitrile functional group in materials (nitrile rubber), natural products (amygdalin), and pharmaceuticals (cyamemazine and citalopram).

to nitrile synthesis that bypasses conventional dehydrating agents and hazardous cyanide-transfer reagents. Electrochemical synthesis has experienced a significant renaissance in recent years, propelled by the growing demand for environmentally responsible, energy-efficient, and reagent-saving chemical processes [18–26].

Electrochemical approaches allow reactions to proceed under comparatively gentle conditions [27], utilize electrical current —ideally derived from renewable sources [28, 29]—as controllable and inherently clean redox input [30, 31], and substantially diminish the generation of hazardous waste relative to conventional stoichiometric oxidizing and reducing agents [32–38]. These advantages have positioned electrosynthesis as a powerful and increasingly indispensable platform in modern organic chemistry [39, 40]. Recent advances highlight the rapidly expanding landscape of electrochemical dehydration strategies (Scheme 2) [41]. Electrochemical access to anhydrides from carboxylic acids [42], the electrodehydrative formation of sulfonyl amidines from sulfonamides [43], and the electrochemical synthesis of esters from carboxylic acids via catalytic dehydration [44] collectively demonstrate the synthetic potential of electric-current-driven water removal. Most recently, electrochemical formation of cyclic anhydrides [45] and in situ generation of sulfonic anhydrides [46] further emphasized the growing importance of the electrochemical dehydration reaction. Despite these advances, electrochemical dehydration of carboxamides to nitriles remains comparatively unexplored, even though such a transformation would provide a direct, scalable, and operationally simple route to nitrile products under environmentally benign conditions.

In this work, an electrochemical dehydration of carboxamides to their corresponding nitriles under mild reaction conditions is reported. The nitriles are formed at ambient conditions and can be easily isolated in high yields. This operationally straightforward method eliminates the need for classical dehydration reagents, diminishes hazardous chemical waste, and provides a safe and scalable alternative for the synthesis of highly value-added nitrile compounds.

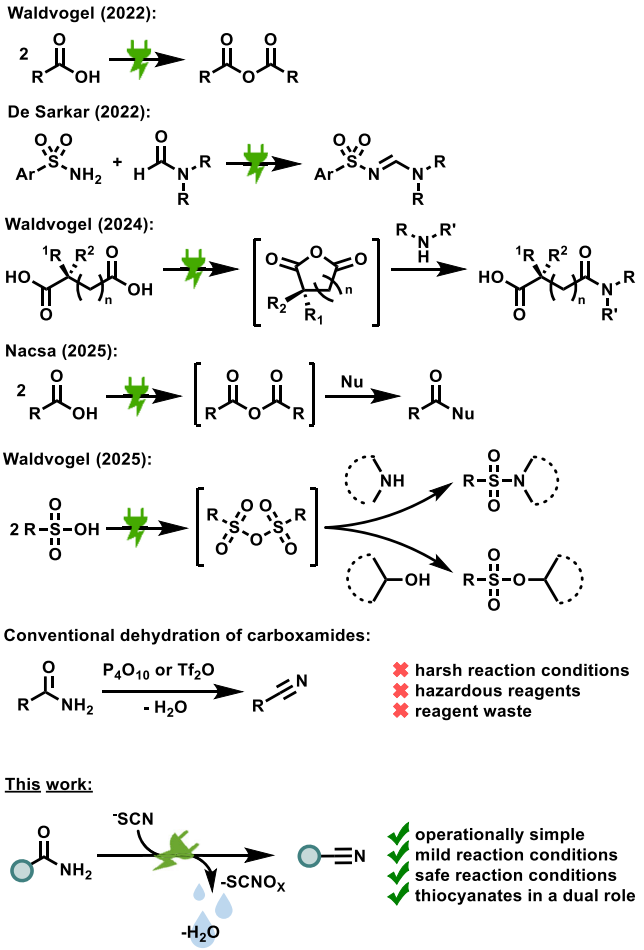

SCHEME 2 | Recent progress in the electrochemical dehydration reaction.

2 | Results and Discussion

Reaction optimization was initiated using conditions previously established within our group for the electrochemical dehydration of carboxylic and sulfonic acids to their corresponding anhydrides in the presence of thiocyanate-based supporting electrolytes [42, 45, 46]. The optimized reaction parameters for the transformation of 2-fluorobenzamide are shown in Scheme 3. Quantitative analysis was performed by ^{19}F NMR spectroscopy using 4-fluorotoluene as an internal standard. Under these optimized conditions (Table 1, entry 1), an NMR yield of 86% was obtained.

To further investigate the influence of electrochemical parameters, the amount of applied charge and current density were systematically varied (Table 1, entries 2 and 3) [47]. Lowering the amount of applied charge to 10 F resulted in a significant decrease in yield to 44% (entry 2), and decreasing the current density to 8.3 mA cm^{-2} likewise led to diminished efficiency (entry 3). The presence and precise amount of 1,1,1,3,3,3-hexafluoro-2-propanol (HFIP) proved to be critical for achieving high yields. Increasing its concentration to 3 vol% resulted in a depressed yield of 42%, while omission of HFIP led to complete loss of product formation (entries 4 and 5). These observations suggest that HFIP likely serves multiple roles in the reaction medium, including acting as a proton source for hydrogen evolution at the cathode, stabilizing radical and ionic intermediates,

10990690, 0, Downloaded from https://chemistry-europe.onlinelibrary.wiley.com/doi/10.1002/ejoc.70328 by Karlsruher Institut Fü¼R, Wiley Online Library on [23/02/2026]. See the Terms and Conditions (https://onlinelibrary.wiley.com/terms-and-conditions) on Wiley Online Library for rules of use; OA articles are governed by the applicable Creative Commons License

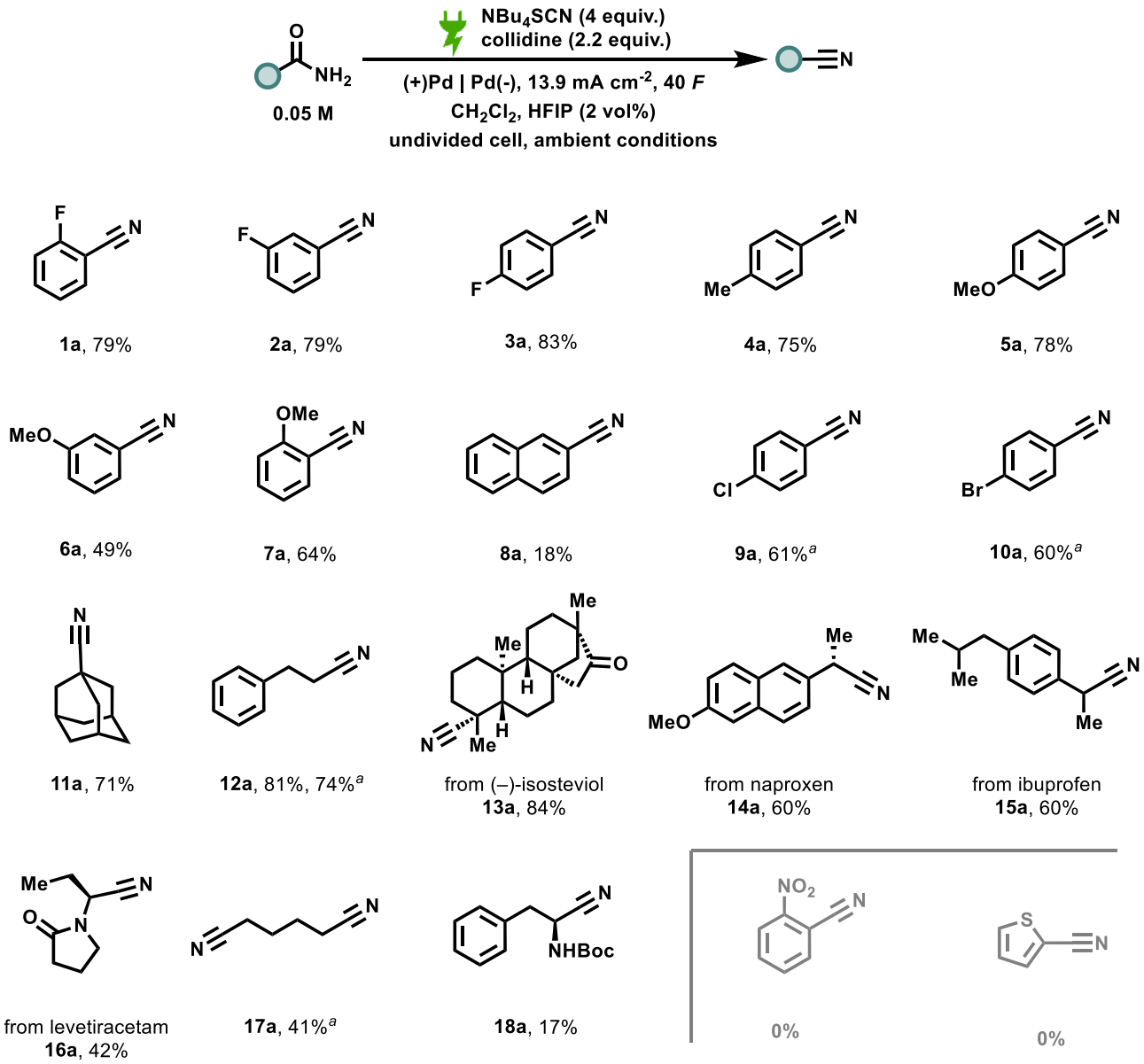

SCHEME 3 | Scope of the carboxamide dehydration reaction. All yields are isolated yields. [a](+)Pt | Pt(−).

and functioning as a cosolvent that enhances electrolyte solubility [48].

Subsequently, the impact of electrode materials on reaction performance was evaluated. The use of platinum as the anodic material afforded a respectable yield of 74% (entry 7), demonstrating its viability as an alternative electrode for broader substrate exploration. However, replacement of NBu_4SCN by KSCN resulted in a dramatically depressed yield of 4% due to the upper cell voltage limit being reached (entry 9), likely a consequence of the poorer solubility of KSCN in the reaction medium. In the absence of NBu_4SCN, no product formation was detected (entry 11). Likewise, control experiments conducted without application of electrical current yielded no traces of the desired product (entry 12), confirming the essential role of electrolysis in promoting this transformation.

With our optimized reaction conditions in hand, the scope of the dehydration reaction was investigated with a range of different carboxamides as starting materials, as shown in Scheme 3. First, aromatic carboxamides were evaluated, giving the corresponding aromatic nitrile in yields up to 83% (**1a** to **10a**). 2-fluorobenzamide as substrate gave the nitrile **1a** in 79% isolated yield, while 3-fluoro- and 4-fluorobenzamide gave nitriles **2a** and **3a** with yields of 79% and 83%, respectively. The similarity in yields for these nitriles shows that the electronic structure of the aromatic ring most likely does not greatly influence the reaction. Similarly, benzamides bearing methoxy-group substituents at different positions at the arene gave **5a**, **6a**, and **7a**, in good yields (78%, 49%, and 64%, respectively). Furthermore, **4a** was isolated in 75% yield. 2-naphthamide gave the corresponding carbonitrile **8a** in a lower yield of 18%. Investigation of the crude reaction mixture with GC–MS techniques showed the possible formation of dimers and deamidation of the starting material, although the precise composition of these species is still under investigation. 4-chlorobenzonitrile **9a** was isolated in 61% yield, while 4-bromobenzonitrile **10a** was obtained in 60% yield, using platinum instead of palladium electrodes for both compounds. Next, aliphatic carboxamides were tested.

10990690, 0, Downloaded from https://chemistry-europe.onlinelibrary.wiley.com/doi/10.1002/ejoc.70328 by Karlsruher Institut Fü¼R, Wiley Online Library on [23/02/2026]. See the Terms and Conditions (https://onlinelibrary.wiley.com/terms-and-conditions) on Wiley Online Library for rules of use; OA articles are governed by the applicable Creative Commons License

TABLE 1 | Optimization of the test reaction.

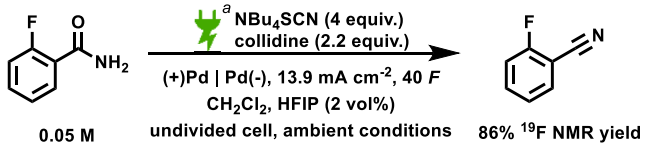

Entry	Deviation from optimal conditions	Yield
1	none	**86%**
2	$F = 10$	44%
3	8.3 mA cm^{-2}	42%
4	HFIP 3 vol%	42%
5	no HFIP	0%
6	MeCN instead of CH_2Cl_2	6%
7	Pt anode	74%
8	2 equiv. NBu_4SCN	44%
9	KSCN instead of NBu_4SCN	4%
10	1.5 equiv 2,4,6-collidine	23%
11	NBu_4BF_4 instead of NBu_4SCN	0%
12	no electricity	0%

Note: Conditions: 2-fluorobenzamide (0.25 mmol, 35 mg, 1 equiv.), NBu_4SCN (1 mmol, 300 mg, 4 equiv.), 2,4,6-collidine (0.55 mmol, 75 µL, 2.2 equiv.), CH_2Cl_2 (5 ml, 0.05 M), HFIP (100 µL, 2 vol%), (+)Pd | Pd(−), 13.9 mA cm^{-2}, 40 *F*, constant current, undivided cell. Yields are reported as ^{19}F NMR yields, using 4-fluorotoluene as internal standard.

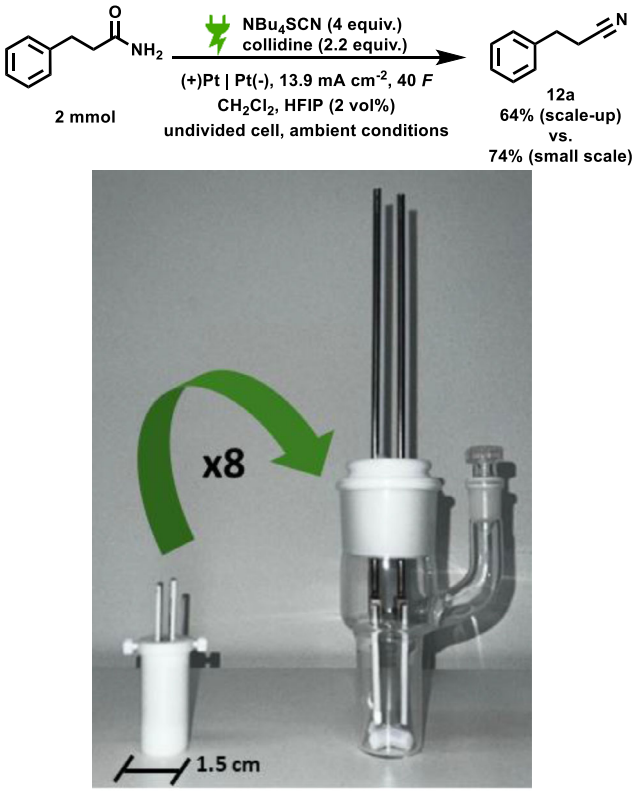

FIGURE 1 | Scale-up reaction.

1-adamantanecarboxamide gave the corresponding tertiary carbonitrile **11a** in 71% yield. Primary carboxamides were also well tolerated, yielding **12a** in 81% yield. When switching to platinum electrodes, nitrile **12a** was isolated in an only slightly lower yield of 74%. We then went on to investigate the reactivity of several carboxamides derived from natural products and pharmaceuticals. Nitrile **13a**, derived from (–)-isosteviol, was isolated in 84% yield. This scaffold has significant importance for affinity materials in sensing applications [49, 50]. Ibuprofen- and naproxen-derived carbonitriles could also be obtained in respectable yields (**14a** and **15a**). The electrochemical dehydration of levetiracetam gave **16a** in a yield of 42%. To assess the reactivity of dicarboxamides, the industrially relevant adiponitrile **17a** was synthesized using our method in a 41% yield from adipamide. Finally, the phenylalanine derived carbonitrile **18a** was isolated in a 17% yield. In this case, the lower yield could be partially explained by the formation of the HFIP ester as a major by-product of the reaction (details provided in the Supporting Information (SI)). Some substrates proved to be unsuccessful, including 2-nitrobenzamide and thiophene-2-carboxamide, likely due to their electrochemical instability toward redox reactions of the substrate backbone.

Demonstrating the scalability of an electrochemical protocol is essential, as it provides a foundation for potential translation to industrial applications. To assess the robustness and scalability of the present electrochemical dehydration reaction, 3-phenylpropan-amide was subjected to electrolysis on an eightfold preparative scale using platinum electrodes to generate 3-phenylpropanenitrile (Figure 1). After standard work-up, the corresponding product **12a** was isolated in 64% yield, which is in line with what we obtained on a small batch. Additional experimental details and operational considerations for the scale-up procedure are provided in the SI.

Although mechanistic investigations have been conducted before for electrochemical dehydration reactions, we performed cyclic voltammetry (CV) measurements to get some insight on the mechanism of this particular chemical transformation. The cyclic voltammogram provides clear insight into the electrochemical behavior of the reaction components and highlights the central role of thiocyanate in the system (Figure 2). The trace corresponding to the supporting electrolyte (purple wave, 0.1 M NBu_4BF_4) shows only background capacitive currents, confirming that no significant faradaic processes occur within the scanned potential window. Neither 2-fluorobenzamide nor collidine introduce appreciable oxidation features, indicating that both species remain electrochemically silent under these conditions and that their oxidation potentials lie outside the accessible range (yellow and black wave). In contrast, the introduction of 40 mM NBu_4SCN generates a distinct anodic wave at ≈1.0 V, which can be attributed to the irreversible oxidation of the thiocyanate anion (green wave). This feature is consistent with oxidation of SCN^- and marks the first substantial faradaic response in the voltammogram. When 2-fluorobenzamide is added together with thiocyanate, the anodic peak increases in intensity and shows a slight shift, suggesting that the oxidized thiocyanate species participate in subsequent chemical steps involving the amide (blue wave). This behavior is characteristic of an EC-type mechanism [51], in which a chemical reaction follows the initial electron-transfer event. The presence of collidine alongside both SCN^- and the amide further amplifies this effect, producing the most pronounced oxidation current and shifting the onset to slightly higher potential. This enhancement indicates that

10990690, 0, Downloaded from https://chemistry-europe.onlinelibrary.wiley.com/doi/10.1002/ejoc.70328 by Karlsruher Institut Fã¼R, Wiley Online Library on [23/02/2026]. See the Terms and Conditions (https://onlinelibrary.wiley.com/terms-and-conditions) on Wiley Online Library for rules of use; OA articles are governed by the applicable Creative Commons License

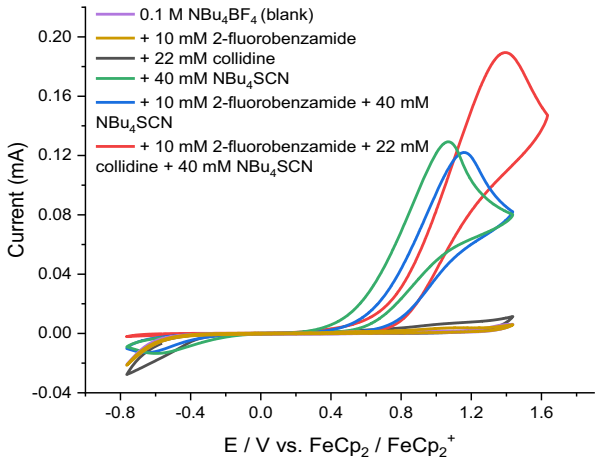

FIGURE 2 | CV experiments. Conditions: in DCM, HFIP (2 vol%), WE: platinum, CE: platinum wire, RE: Ag/Ag^+, scan rate: 100 mV/s. CV = Cyclic voltammetry.

collidine facilitates downstream chemical steps—likely through proton transfer or stabilization of reactive intermediates—which in turn increases the turnover of the oxidized thiocyanate species. Overall, the CV data strongly support a mediated oxidation process, in which thiocyanate serves as the redox-active species, while the amide and collidine modulate the efficiency of the subsequent chemical steps that drive the overall electrochemical transformation.

With the data provided by the CV experiments, we propose a mechanism for the electrochemical dehydration reaction of carboxamides.

The proposed electrochemical mechanism for the dehydration of carboxamides to their corresponding nitriles is shown in Scheme 4. At the anode, the thiocyanate-based mediator **I** ($X^- = SCN^-$, $OSCN^-$, or O_2SCN^-) undergoes a two-electron oxidation to generate the reactive species **II** X^+, which subsequently engages in a sequence of chemical steps with the carboxamide substrate **III**. The oxidized mediator interacts with the amide to form an activated O-acyl intermediate **IV** through nitrogen-centered activation and proton-transfer processes facilitated by the base (B/BH^+). This sequence ultimately generates a highly activated intermediate that eliminates species **V** and collapses to the nitrile **VI** (R–C≡N). At the cathode, proton reduction occurs generating molecular hydrogen and closing the overall redox balance of the system. Together, these steps illustrate a mediated electrochemical pathway, in which thiocyanate species enable efficient oxidative dehydration under mild conditions.

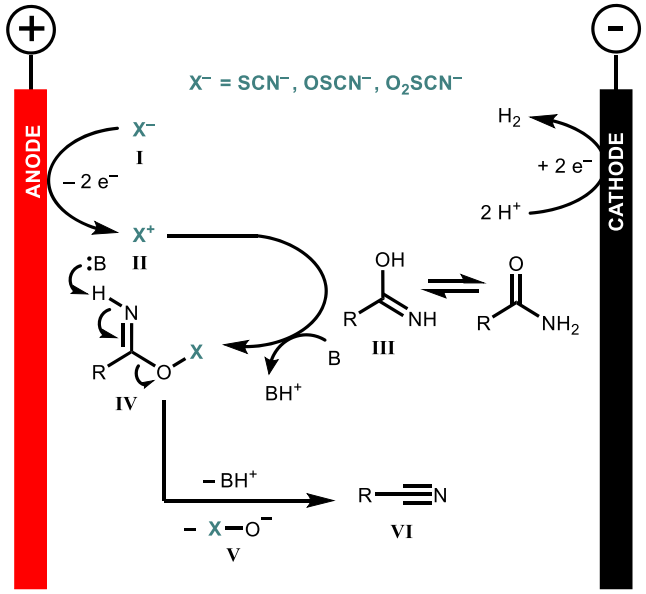

SCHEME 4 | Proposed mechanism.

3 | Conclusion

In summary, we have established a practical and efficient electrochemical method for the dehydration of carboxamides to their corresponding nitriles under mild and operationally simple conditions. This procedure eliminates the need for classical stoichiometric dehydrating agents and hazardous cyano-transfer reagents, thereby offering a safer and more sustainable alternative for accessing nitrile functionalities. Systematic optimization, which yielded **1a** in 86% ^{19}F NMR yield, revealed the essential role of thiocyanate as a redox mediator and the critical contribution of HFIP to reaction efficiency, insights that were further supported by CV studies. The electroanalytical data indicate a mediated anodic oxidation mechanism, in which the thiocyanate species facilitate the key activation steps, leading to nitrile formation. Across a scope of 18 examples, the reaction exhibited broad functional-group tolerance and delivered isolated yields of up to 84%. Moreover, it can be scaled up with minimal loss in efficiency (64% vs. 74% isolated yield), underscoring its robustness and potential applicability beyond laboratory conditions. Overall, this study expands the scope of electrochemical dehydration chemistry and provides a valuable, environmentally conscious platform for the synthesis of nitrile-containing molecules.

Acknowledgments

The authors are grateful for funding by Deutsche Forschungsgemeinschaft (German Research Foundation) under Germany's Excellence Strategy—EXC-2033-390677874-RESOLV.

Open Access funding enabled and organized by Projekt DEAL.

Funding

This work was supported by Deutsche Forschungsgemeinschaft (Germany's Excellence Strategy—EXC-2033-390677874-RESOLV), Max-Planck-Gesellschaft (Open Access by DEAL Agreement).

Conflicts of Interest

The authors declare no conflicts of interest.

Data Availability Statement

The data that support the findings of this study are available in the SI of this article.

References

1. X. Wang, Y. Wang, X. Li, Z. Yu, C. Song, and Y. Du, "Nitrile-Containing Pharmaceuticals: Targets, Mechanisms of Action, and Structure–Activity Relationship Studies," *RSC Medicinal Chemistry* 12 (2021): 1650–1671.

10990690, 0, Downloaded from https://chemistry-europe.onlinelibrary.wiley.com/doi/10.1002/ejoc.70328 by Karlsruher Institut Fü4R, Wiley Online Library on [23/02/2026]. See the Terms and Conditions (https://onlinelibrary.wiley.com/terms-and-conditions) on Wiley Online Library for rules of use; OA articles are governed by the applicable Creative Commons License

2. C. Scotti and J. W. Barlow, "Natural Products Containing the Nitrile Functional Group and Their Biological Activities," *Natural Product Communications* 17 (2022): 1934578X221099973.

3. R. Narobe, M. N. Perner, M. D. J. Gálvez-Vázquez, et al., "Practical Electrochemical Hydrogenation of Nitriles at the Nickel Foam Cathode," *Green Chemistry* 26 (2024): 10567–10574.

4. R. Narobe, M. N. Perner, S. Ulrich, et al., "Scalable Electrochemical Preparation of Spermidine and Spermine," *ACS Electrochemistry* 2025).

5. J.-T. Yu, F. Teng, and J. Cheng, "The Construction of X–CN (X=N, S, O) Bonds," *Advanced Synthesis & Catalysis* 359 (2017): 26–38.

6. M. Ganesan and P. Nagaraaj, "Recent Developments in Dehydration of Primary Amides to Nitriles," *Organic Chemistry Frontiers* 7 (2020): 3792–3814.

7. R. V. Jagadeesh, H. Junge, and M. Beller, "Green Synthesis of Nitriles Using Non-Noble Metal Oxides-Based Nanocatalysts," *Nature Communications* 5 (2014): 4123.

8. M. Neetha, C. M. A. Afsina, T. Aneeja, and G. Anilkumar, "Recent Advances and Prospects in the Palladium-Catalyzed Cyanation of Aryl Halides," *RSC Advances* 10 (2020): 33683–33699.

9. C. Xian, J. He, Y. He, et al., "High Nitrile Yields of Aerobic Ammoxidation of Alcohols Achieved by Generating •O2– and Br• Radicals over Iron-Modified TiO2 Photocatalysts," *Journal of the American Chemical Society* 144 (2022): 23321–23331.

10. S. Zhou, K. Junge, D. Addis, S. Das, and M. Beller, "A General and Convenient Catalytic Synthesis of Nitriles from Amides and Silanes," *Organic Letters* 11 (2009): 2461–2464.

11. M. F. Hartmer and S. R. Waldvogel, "Electroorganic Synthesis of Nitriles via a Halogen-free Domino Oxidation–reduction Sequence," *Chemical Communications* 51 (2015): 16346–16348.

12. C. Gütz, V. Grimaudo, M. Holtkamp, et al., "Leaded Bronze: An Innovative Lead Substitute for Cathodic Electrosynthesis," *ChemElectroChem* 5 (2018): 247–252.

13. M. Hinzmann, H. Yavuzer, M. Bittmann, and H. Gröger, "Novel Approach Toward Industrial Aromatic Nitriles via Biocatalysis: From Rational Enzyme Design to Sustainable, Energy-Saving Technology Platform," *Chem Catalysis* 3 (2023): 100572.

14. H. Gröger and Y. Asano, "Cyanide-Free Enantioselective Catalytic Strategies for the Synthesis of Chiral Nitriles," *The Journal of Organic Chemistry* 85 (2020): 6243–6251.

15. C. Plass, A. Hinzmann, M. Terhorst, et al., "Approaching Bulk Chemical Nitriles from Alkenes: A Hydrogen Cyanide-Free Approach through a Combination of Hydroformylation and Biocatalysis," *ACS Catalysis* 9 (2019): 5198–5203.

16. D. F. Nater, P. Hendriks, and S. R. Waldvogel, "Electrochemical Hofmann Rearrangement at High Current Densities in a Simple Flow Setup," *Molecular Catalysis* 554 (2024): 113823.

17. D. F. Nater, R. Zhao, J. Rocker, et al., "Hectogram-Scale Synthesis of Carbamates Using Electrochemical Hofmann Rearrangement in Flow," *Organic Process Research & Development* 29 (2025): 2370–2377.

18. S. R. Waldvogel and B. Janza, "Renaissance Elektrochemischer Methoden Zum Aufbau komplexer Moleküle," *Angewandte Chemie* 126 (2014): 7248–7249.

19. S. R. Waldvogel and B. Janza, "Renaissance of Electrosynthetic Methods for the Construction of Complex Molecules," *Angewandte Chemie, International Edition* 53 (2014): 7122–7123.

20. M. D. Kärkäs, Electrochemical Strategies for C–H Functionalization and C–N Bond Formation," *Chemical Society Reviews* 47 (2018): 5786–5865.

21. A. Shatskiy, H. Lundberg, and M. D. Kärkäs, "Organic Electrosynthesis: Applications in Complex Molecule Synthesis," *ChemElectroChem* 6 (2019): 4067–4092.

22. C. Zhu, N. W. J. Ang, T. H. Meyer, Y. Qiu, and L. Ackermann, "Organic Electrochemistry: Molecular Syntheses with Potential," *ACS Central Science* 7 (2021): 415–431.

23. M. C. Leech and K. Lam, "A Practical Guide to Electrosynthesis," *Nature Reviews Chemistry* 6 (2022): 275–286.

24. Z. Zhong, Y. Liu, L. Liao, and J.-P. Wan, "Electrochemical Annulation of p-Alkoxy or p-Hydroxy Anilines with Enaminones for Selective Indole and Benzofuran Synthesis," *Organic Letters* 27 (2025): 2537–2541.

25. P. Ryan, D. Bhattacherjee, T. Wirth, L. Hunter, and G. Pascali, "Electrochemical Fluorination of Proline Derivatives," *European Journal of Organic Chemistry* 28 (2025): e202500264.

26. Q. Huang, J. Liu, and J.-P. Wan, "Electrochemical Enaminone-Thioamide Annulation and Thioamide Dimeric Annulation for the Tunable Synthesis of Thiazoles and 1,2,4-Thiadiazole, *Organic Letters* 26 (2024): 5263–5268.

27. J. Seidler, J. Strugatchi, T. Gärtner, and S. R. Waldvogel, "Does Electrifying Organic Synthesis Pay Off? The Energy Efficiency of Electro-organic Conversions," *MRS Energy & Sustainability : A Review Journal* 7 (2020): E42.

28. A. Wiebe, T. Gieshoff, S. Möhle, E. Rodrigo, M. Zirbes, and S. R. Waldvogel, "Elektrifizierung der Organischen Synthese," *Angewandte Chemie* 130 (2018): 5694–5721.

29. A. Wiebe, T. Gieshoff, S. Möhle, E. Rodrigo, M. Zirbes, and S. R. Waldvogel, "Electrifying Organic Synthesis," *Angewandte Chemie, International Edition* 57 (2018): 5594–5619.

30. S. B. Beil, D. Pollok, and S. R. Waldvogel, "Reproduzierbarkeit in elektroorganischer Synthese – Mythen und Missverständnisse," *Angewandte Chemie* 133 (2021): 14874–14883.

31. S. B. Beil, D. Pollok, and S. R. Waldvogel, "Reproducibility in Electroorganic Synthesis—Myths and Misunderstandings," *Angewandte Chemie, International Edition* 60 (2021): 14750–14759.

32. S. Möhle, M. Zirbes, E. Rodrigo, T. Gieshoff, A. Wiebe, and S. R. Waldvogel, "Moderne Aspekte Der Elektrochemie Zur Synthese Hochwertiger Organischer Produkte," *Angewandte Chemie* 130 (2018): 6124–6149.

33. S. Möhle, M. Zirbes, E. Rodrigo, T. Gieshoff, A. Wiebe, and S. R. Waldvogel, "Modern Electrochemical Aspects for the Synthesis of Value-Added Organic Products," *Angewandte Chemie, International Edition* 57 (2018): 6018–6041.

34. B. K. Peters, K. X. Rodriguez, S. H. Reisberg, et al., "Scalable and Safe Synthetic Organic Electroreduction Inspired by Li-Ion Battery Chemistry," *Science* 363 (2019): 838–845.

35. S. R. Waldvogel, S. Lips, M. Selt, B. Riehl, and C. J. Kampf, "Electrochemical Arylation Reaction," *Chemical Reviews* 118 (2018): 6706–6765.

36. J. L. Röckl, D. Pollok, R. Franke, and S. R. Waldvogel, "A Decade of Electrochemical Dehydrogenative C,C-Coupling of Aryls," *Accounts of Chemical Research* 53 (2020): 45–61.

37. J. Kulisch, M. Nieger, F. Stecker, A. Fischer, and S. R. Waldvogel, "Effiziente und Stereodivergierende Elektrochemische Synthese von Optisch Reinen Menthylaminen," *Angewandte Chemie* 123 (2011): 5678–5682.

38. J. Kulisch, M. Nieger, F. Stecker, A. Fischer, and S. R. Waldvogel, "Efficient and Stereodivergent Electrochemical Synthesis of Optically Pure Menthylamines," *Angewandte Chemie, International Edition* 50 (2011): 5564–5567.

39. R. D. Little and K. D. Moeller, "Introduction: Electrochemistry: Technology, Synthesis, Energy, and Materials," *Chemical Reviews* 118 (2018): 4483–4484.

40. D. Pollok and S. R. Waldvogel, "Electro-Organic Synthesis – a 21st Century Technique," *Chemical Science* 11 (2020): 12386–12400.

10990690, 0, Downloaded from https://chemistry-europe.onlinelibrary.wiley.com/doi/10.1002/ejoc.70328 by Karlsruher Institut Fï¾¼R, Wiley Online Library on [23/02/2026]. See the Terms and Conditions (https://onlinelibrary.wiley.com/terms-and-conditions) on Wiley Online Library for rules of use; OA articles are governed by the applicable Creative Commons License

41. J. Schneider, E. Lunghi, and S. R. Waldvogel, "Electrochemical Dehydration Reaction," *ChemSusChem* 18 (2025): e202501552.

42. A. P. Häring, D. Pollok, B. R. Strücker, V. Kilian, J. Schneider, and S. R. Waldvogel, "Beyond Kolbe and Hofer–Moest: Electrochemical Synthesis of Carboxylic Anhydrides from Carboxylic Acids," *ChemistryOpen* 11 (2022): e202200059.

43. K. Mahanty, A. Halder, and S. De Sarkar, "Synthesis of N-Sulfonyl Amidines and 1,3,4-Oxadiazoles through Electrochemical Activation of DMF," *Advanced Synthesis & Catalysis* 365 (2023): 96–103.

44. J. Han, J. J. Piane, H. Gizenski, E. Elacqua, and E. D. Nacsa, "An Electrochemical Design for a General Catalytic Carboxylic Acid Substitution Platform via Anhydrides at Room Temperature: Amidation, Esterification, and Thioesterification," *Organic Letters* 27 (2025): 1923–1928.

45. J. Schneider, A. P. Häring, and S. R. Waldvogel, "Electrochemical Dehydration of Dicarboxylic Acids to Their Cyclic Anhydrides," *Chemistry - A European Journal* 30 (2024): e202400403.

46. E. Lunghi, A. M. van Koten, J. Schneider, and S. R. Waldvogel, "Electrochemical Dehydration of Sulfonic Acids to Their Anhydrides," *The Journal of Organic Chemistry* 90 (2025): 12259–12264.

47. M. Dörr, M. M. Hielscher, J. Proppe, and S. R. Waldvogel, "Electrosynthetic Screening and Modern Optimization Strategies for Electrosynthesis of Highly Value-added Products," *ChemElectroChem* 8 (2021): 2621–2629.

48. J. L. Röckl, M. Dörr, and S. R. Waldvogel, "Electrosynthesis 2.0 in 1,1,1,3,3,3-Hexafluoroisopropanol/Amine Mixtures," *ChemElectroChem* 7 (2020): 3686–3694.

49. C. Lohoelter, M. Brutschy, D. Lubczyk, and S. R. Waldvogel, "Novel Supramolecular Affinity Materials Based on (−)-Isosteviol as Molecular Templates," *Beilstein Journal of Organic Chemistry* 9 (2013): 2821–2833.

50. C. Lohoelter, M. Weckbecker, and S. R. Waldvogel, "(−)-Isosteviol as a Versatile Ex-Chiral-Pool Building Block for Organic Chemistry," *European Journal of Organic Chemistry* 2013 (2013): 5539–5554.

51. C. Sandford, M. A. Edwards, K. J. Klunder, et al., "A Synthetic Chemist's Guide to Electroanalytical Tools for Studying Reaction Mechanisms," *Chemical Science* 10 (2019): 6404–6422.

Supporting Information

Supporting Fig. S1: Undivided screening setup similar to the setup available from IKA (left) and undivided cell equipped with palladium foil as anode and cathode (right)[5]. **Supporting Fig. S2:** 50 mL undivided cell with glassy carbon anode and platinum cathode and electrode holders used for the scale-up. **Supporting Fig. S3:** Typical ^{19}F NMR spectrum in $CDCl_3$ of a reaction mixture used for quantification of **1a**[2]. **Supporting Fig. S4:** Cyclic voltammogram of 0.1 mol/L NBu_4BF_4 in CH_2Cl_2/HFIP (2 vol%) (purple curve), addition of 2-fluorobenzamide 0.01 mol/L (orange curve). CV of collidine 0.022 mol/L in NBu_4BF_4 (black curve), CV of NBu_4SCN 0.04 mol/L in NBu_4BF_4 (green curve). CV of 2-fluorobenzamide 0.01 mol/L and NBu4SCN 0.04 mol/L in NBu_4BF_4 (blue curve), addition of collidine 0.022 mol/L (red curve). Ag^+/Ag reference electrode (RE), platinum as working electrode (WE), and platinum wire as counter electrode (CE). Each CV measurement was referenced against ferrocene. Oxidation potentials are marked and displayed as the half-wave potential of the respective peak (IUPAC convention). Scan has been taken in this direction: 0 V → + 2.0/2.2 V → −0.2 V → 0 V, with a scan rate of 100 mV/s. **Supporting Fig. S5:** Cyclic voltammogram of 0.1 mol/L NBu_4BF_4 in CH_2Cl_2/HFIP (2 vol%) (blue curve), addition of 2-fluorobenzonitrile 0.01 mol/L (black curve). CV of 2-fluorobenzamide 0.01 mol/L in NBu_4BF_4 (green curve), CV of NBu_4SCN 0.04 mol/L in NBu_4BF_4 (red curve). Ag^+/Ag RE, platinum as WE, and platinum wire as CE. Each CV measurement was referenced against ferrocene. Oxidation potentials are marked and displayed as the half-wave potential of the respective peak (IUPAC convention). Scan has been taken in this direction: 0 V → +2.0 V→−0.2 V→ 0 V, with a scan rate of 100 mV/s. **Supporting Fig. S6:** Unsuccessful substrates. **Supporting Fig. S7:** ^1H NMR spectrum (400 MHz, 25°C, $CDCl_3$) of **13**. **Supporting Fig. S8:** $^{13}C\{^1H\}$ NMR spectrum (101 MHz, 25°C, $CDCl_3$) of **13**. **Supporting Fig. S9:** ^1H NMR spectrum (400 MHz, 25°C, $CDCl_3$) of **14**. **Supporting Fig. S10:** $^{13}C\{^1H\}$ NMR spectrum (101 MHz, 25°C, $CDCl_3$) of **14**. **Supporting Fig. S11:** ^1H NMR spectrum (400 MHz, 25°C, $CDCl_3$) of **15**. **Supporting Fig. S12:** $^{13}C\{^1H\}$ NMR spectrum (101 MHz, 25°C, $CDCl_3$) of **15**. **Supporting Fig. S13:** ^1H NMR spectrum (400 MHz, 25°C, $CDCl_3$) of **18**. **Supporting Fig. S14:** $^{13}C\{^1H\}$ NMR spectrum (101 MHz, 25°C, $CDCl_3$) of **18**. **Supporting Fig. S15:** ^1H NMR spectrum (400 MHz, 25°C, $CDCl_3$) of **1a**. **Supporting Fig. S16:** $^{13}C\{^1H\}$ NMR spectrum (101 MHz, 25°C, CDCl3) of **1a**. **Supporting Fig. S17:** ^{19}F NMR spectrum (376 MHz, 25°C, $CDCl_3$) of **1a**. **Supporting Fig. S18:** ^1H NMR spectrum (400 MHz, 25°C, $CDCl_3$) of **2a**. **Supporting Fig. S19:** $^{13}C\{^1H\}$ NMR spectrum (101 MHz, 25°C, $CDCl_3$) of **2a**. **Supporting Fig. S20:** ^{19}F NMR spectrum (376 MHz, 25°C, $CDCl_3$) of **2a**. **Supporting Fig. S21:** ^1H NMR spectrum (400 MHz, 25°C, $CDCl_3$) of **3a**. **Supporting Fig. S22:** $^{13}C\{^1H\}$ NMR spectrum (101 MHz, 25°C, $CDCl_3$) of **3a**. **Supporting Fig. S23:** ^{19}F NMR spectrum (376 MHz, 25°C, $CDCl_3$) of **3a**. **Supporting Fig. S24:** ^1H NMR spectrum (400 MHz, 25°C, $CDCl_3$) of **4a**. **Supporting Fig. S25:** $^{13}C\{^1H\}$ NMR spectrum (101 MHz, 25°C, $CDCl_3$) of **4a**. **Supporting Fig. S26:** ^1H NMR spectrum (400 MHz, 25°C, $CDCl_3$) of **5a**. **Supporting Fig. S27:** $^{13}C\{^1H\}$ NMR spectrum (101 MHz, 25°C, $CDCl_3$) of **5a**. **Supporting Fig. S28:** ^1H NMR spectrum (400 MHz, 25°C, $CDCl_3$) of **6a**. **Supporting Fig. S29:** $^{13}C\{^1H\}$ NMR spectrum (101 MHz, 25°C, $CDCl_3$) of **6a**. **Supporting Fig. S30:** ^1H NMR spectrum (400 MHz, 25°C, $CDCl_3$) of **7a**. **Supporting Fig. S31:** $^{13}C\{^1H\}$ NMR spectrum (101 MHz, 25°C, $CDCl_3$) of **7a**. **Supporting Fig. S32:** ^1H NMR spectrum (400 MHz, 25°C, $CDCl_3$) of **8a**. **Supporting Fig. S33:** $^{13}C\{^1H\}$ NMR spectrum (101 MHz, 25°C, $CDCl_3$) of **8a**. **Supporting Fig. S34:** ^1H NMR spectrum (400 MHz, 25°C, $CDCl_3$) of **9a**. **Supporting Fig. S35:** $^{13}C\{^1H\}$ NMR spectrum (101 MHz, 25°C, $CDCl_3$) of **9a**. **Supporting Fig. S36:** ^1H NMR spectrum (400 MHz, 25°C, $CDCl_3$) of **10a**. **Supporting Fig. S37:** $^{13}C\{^1H\}$ NMR spectrum (101 MHz, 25°C, $CDCl_3$) of **10a**. **Supporting Fig. S38:** ^1H NMR spectrum (400 MHz, 25°C, $CDCl_3$) of 11a. **Supporting Fig. S39:** $^{13}C\{^1H\}$ NMR spectrum (101 MHz, 25°C, $CDCl_3$) of 11a. **Supporting Fig. S40:** ^1H NMR spectrum (400 MHz, 25°C, $CDCl_3$) of **12a**. **Supporting Fig. S41:** $^{13}C\{^1H\}$ NMR spectrum (101 MHz, 25°C, $CDCl_3$) of **12a**. **Supporting Fig. S42:** ^1H NMR spectrum (400 MHz, 25°C, $CDCl_3$) of 13a. **Supporting Fig. S43:** $^{13}C\{^1H\}$ NMR spectrum (101 MHz, 25°C, $CDCl_3$) of **13a**. **Supporting Fig. S44:** ^1H NMR spectrum (400 MHz, 25 °C, $CDCl_3$) of **14a**. **Supporting Fig. S45:** $^{13}C\{^1H\}$ NMR spectrum (101 MHz, 25°C, $CDCl_3$) of **14a**. **Supporting Fig. S46:** ^1H NMR spectrum (400 MHz, 25°C, $CDCl_3$) of **15a**. **Supporting Fig. S47:** $^{13}C\{^1H\}$ NMR spectrum (101 MHz, 25°C, $CDCl_3$) of **15a**. **Supporting Fig. S48:** ^1H NMR spectrum (400 MHz, 25°C, $CDCl_3$) of **16a**. **Supporting Fig. S49:** $^{13}C\{^1H\}$ NMR spectrum (101 MHz, 25°C, $CDCl_3$) of **16a**. **Supporting Fig. S50:** ^1H NMR spectrum (400 MHz, 25°C, $CDCl_3$) of **17a**. **Supporting Fig. S51:** $^{13}C\{^1H\}$ NMR spectrum (101 MHz, 25°C, $CDCl_3$) of **17a**. **Supporting Fig. S52:** ^1H NMR spectrum (400 MHz, 25°C, $CDCl_3$) of **18a**. **Supporting Fig. S53:** $^{13}C\{^1H\}$ NMR spectrum (101 MHz, 25°C, $CDCl_3$) of **18a**. **Supporting Fig. S54:** ^1H NMR spectrum (400 MHz, 25°C, $CDCl_3$) of the HFIP ether by-product resulting from the electrochemical dehydration of compound 18. **Supporting Table S1:** Electrode materials, specification, and supplier. **Supporting Table S2:** First experiments. **Supporting Table S3:** Screening of cathodic material. **Supporting Table S4:** Screening of anodic material. **Supporting Table S5:** Screening of current density. **Supporting Table S6:** Screening of supporting electrolytes. **Supporting Table S7:** Screening of supporting electrolyte concentration. **Supporting Table S8:** Screening of solvents. **Supporting Table S9:** Screening of the HFIP volume %. **Supporting Table S10:** Screening of base. **Supporting Table S11:** Screening of amount of base. **Supporting Table S12:** Screening of amount of charge. **Supporting Table S13:** Final optimized reaction conditions. **Supporting Table S14:** Control experiments.

10990690, 0, Downloaded from https://chemistry-europe.onlinelibrary.wiley.com/doi/10.1002/ejoc.70328 by Karlsruher Institut Fü¼R, Wiley Online Library on [23/02/2026]. See the Terms and Conditions (https://onlinelibrary.wiley.com/terms-and-conditions) on Wiley Online Library for rules of use; OA articles are governed by the applicable Creative Commons License